PRECIPITATION PROCESSES IN Mg-Y-Nd-Ag ALLOYS SUITABLE FOR BIODEGRADABLE IMPLANTS

Marián VLČEK[a], František LUKÁČ[a], Ivana STULÍKOVÁ[a], Bohumil SMOLA[a], Hana KUDRNOVÁ[a], Martin VLACH[a], Veronika KODETOVÁ[a], Gábor SZAKÁCS[b], Norbert HORT[b], Karl Ulrich KAINER[b]

[a] *Faculty of Mathematics and Physics, Charles University in Prague, Prague, Czech Republic, EU,* marian.vlcek@gmail.com

[b] *Institute for Material Research, Helmholtz-Zentrum Geesthacht, Geesthacht, Germany, EU*

Abstract

Biodegradable magnesium implants show great promise in improving quality of healthcare and reduction of costs by removing the necessity of a second surgery. In this work we study novel Mg-Y-Nd-Ag-based materials (total solute content less than 7 wt.%) envisaged for biodegradable implants. Studied alloys were subjected to isochronal annealing in as cast condition and also after homogenization annealing. Physical properties and precipitation processes in these alloys were investigated by optical microscopy, transmission and scanning electron microscopy, differential scanning calorimetry, electrical resistometry and by microhardness measurements. Our results were compared to the precipitation processes identified in the WE43 alloy.

Keywords: Biodegradable implants, magnesium alloys, heat treatment

1. INTRODUCTION

Biodegradable magnesium implants show great promise in improving quality of healthcare and reduction of costs by removing the necessity of a second surgery [1]. The WE43 (Mg-Y-RE-Zr) alloy originally designed for high-temperature applications was recently used as candidate material for biodegradable implants. Furthermore, silver was identified as suitable alloying element for biodegradable magnesium alloys due to its antibacterial properties [2]. Knowledge of microstructure and mechanical properties development with increasing temperature is very important also for applications at ambient temperature, because it determinates Mg-alloys production procedures requiring elevated temperatures. Supersaturated solid solution can be produced by annealing at suitable temperature and subsequent quenching. With increasing temperature, supersaturated solid solution will decompose through sequence of metastable phases until thermodynamically stable phase is formed. According to the composition of studied alloys, there are two precipitation sequences which might in principle proceed in them: Mg-Y-Nd sequence [3]

$\alpha^{'}(\mathrm{hcp}) \rightarrow \beta^{''}(\mathrm{D0_{19}\ clusters}) \rightarrow \beta^{''}(\mathrm{D0_{19}\ plates}) \rightarrow \beta^{'}(\mathrm{cbco}) \rightarrow \beta_1(\mathrm{fcc, Mg_3Gd\ type}) \rightarrow \beta\,(\mathrm{fcc, Mg_5Gd\ type}) \rightarrow \beta\,(\mathrm{bct, Mg_{41}Nd_5\ type})$ and Mg-Ag-Nd sequence [4]

$\alpha^{'} \rightarrow \mathrm{GP\ zones\ (rod\text{-}like)} \rightarrow \gamma\ (\mathrm{hexagonal\ rods}) \rightarrow \beta\ (\mathrm{hexagonal\ equiaxed}) \rightarrow \mathrm{Mg_{12}Nd_2Ag\ (hexagonal)}$ $\alpha^{'} \rightarrow \mathrm{GP\ zones\ (ellipsoidal)} \rightarrow \beta\ (\mathrm{hexagonal\ equiaxed}) \rightarrow \mathrm{Mg_{12}Nd_2Ag\ (hexagonal)}$.

2. EXPERIMENTAL DETAILS

Samples of Mg-Y-Nd-Ag with compositions Mg-2.0 wt.% Y-0.7 wt.% Nd-1.0 wt.% Ag (WEQ211) and Mg-3.7 wt.% Y-2.1 wt.% Nd-0.9 wt.% Ag (WEQ421) were prepared by gravity casting under protective atmosphere. Samples of WEQ211 alloy were homogenized at 500 °C/90 min and samples of WEQ421 alloy at 500 °C/30 min. As cast and homogenized samples were subjected to isochronal annealing with step 20 K/20 min. Each annealing step was finished by quenching into the water of room temperature. Electrical resistivity was measured at 77 K by the DC four-point method with a dummy specimen in series. The influence of parasitic thermo-electromotive force was suppressed by current reversal. Relative electrical resistivity changes $\Delta\rho/\rho_0$ were obtained to within an accuracy of 10^{-4} (ρ_0 is the value of resistivity in the initial state). Vickers hardness (HV) was measured at room temperature on polished samples using microhardness tester Struers Duramin 300 using the load of 100 g applied for 10 s. Each hardness measurement was repeated at least ten times to improve precision of measurement and estimate statistical uncertainty of the hardness value. Differential scanning calorimetry (DSC) measurements of as cast specimens were performed at heating rate 10 K/min using the Netsch DSC 200 F3 apparatus with Al_2O_3 pans. Measurements were performed without a reference specimen. Nitrogen flow of 40 ml/min was used as a protective atmosphere. Scanning electron microscopy (SEM) was performed on Tescan MIRA I equipped with Bruker EDX analyzer. Transmission electron microscopy (TEM) investigations were carried out using JEOL JEM 2000FX electron microscope.

3. RESULTS

As cast samples of WEQ211 and WEQ421 alloys were polished and etched in 1 % Nital for 15 s and subsequently examined by optical microscopy. Average grain sizes in as cast WEQ211 and WEQ421 alloys were determined as ~200 μm and ~275 μm, respectively. Examination of microstructure of as cast WEQ421 alloy by SEM revealed presence of secondary phases and inhomogeneous distribution of solute elements. This can be clearly seen from SEM image in **Fig. 1a**. Energy dispersive X-ray spectroscopy (EDX) revealed enhanced concentration of Y and Nd in the particles and consequently lower that average concentration of alloying elements in the matrix.

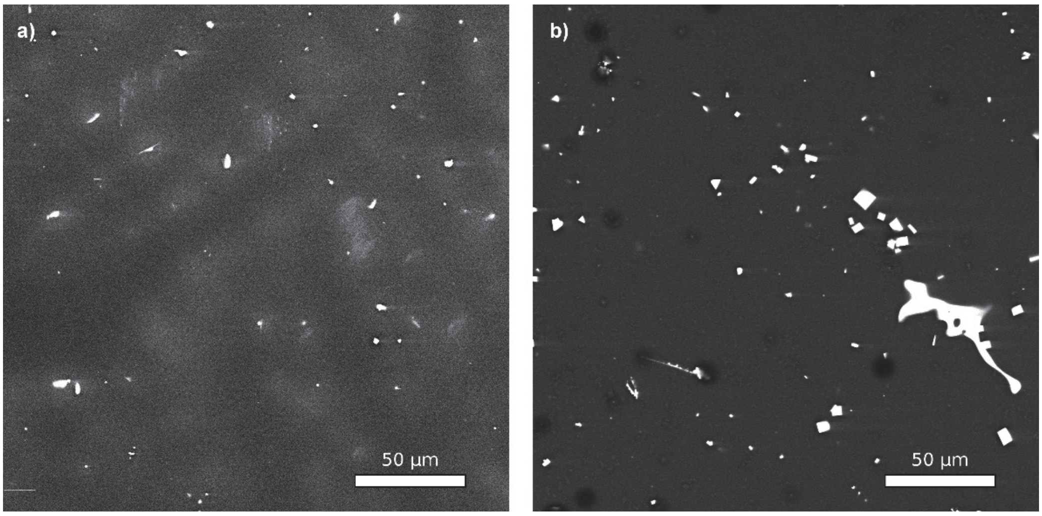

Fig. 1 SEM images of WEQ421 alloy: a) as cast, b) homogenized 500 °C/7 hours

Results of TEM investigations of as cast WEQ421 alloy are shown in **Fig. 2**. Stacking faults were observed by TEM (**Fig. 2a**) and structure of secondary phase(s) from **Fig. 1a** was identified as Mg_5Gd-type by selected area electron diffraction (SAED) (see **Fig. 2b**). Microstructure characterization of WEQ211 alloy [5] revealed presence of grain boundary phases and also inhomogeneous distribution of solute elements in as cast condition. Furthermore, long-period stacking-ordered (LPSO) structures of 18R type were identified in the as cast WEQ211 alloy [5] which were not observed in as cast WEQ421 alloy.

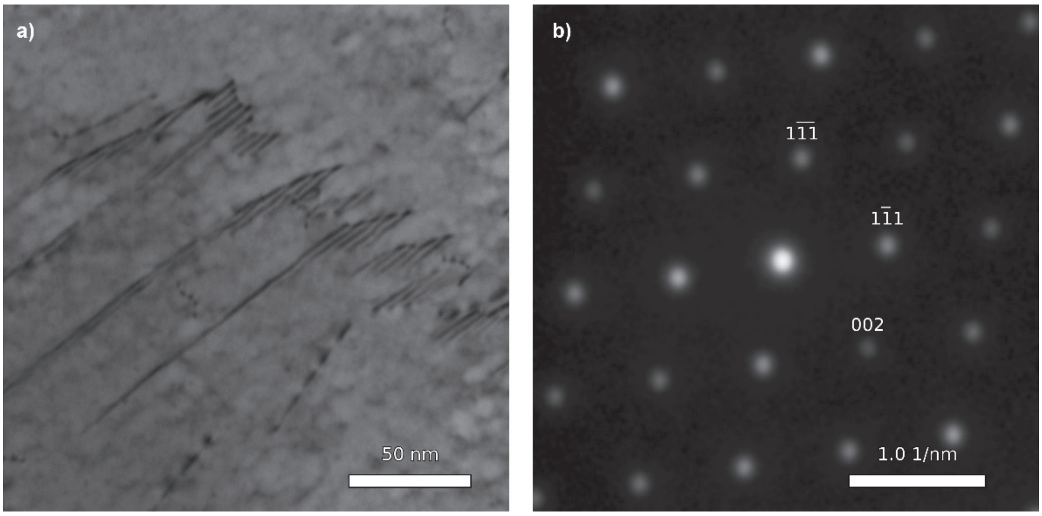

Fig. 2 TEM of as cast WEQ421 alloy: a) stacking faults (bright field), b) SAED of Mg_5Gd type particle in [110] zone

Results of HV measurements and relative resistivity changes of as cast WEQ211 and WEQ421 samples during isochronal annealing are shown in **Fig. 3**. Electrical resistivity of as cast WEQ211 alloy significantly increases in the temperature range from 160 °C to 300 °C. Local minimum of resistivity was observed at 380 °C after which resistivity increases and reaches maximum at 500 °C. Evolution of microhardness with annealing temperature shows dip in hardness at 120 °C while electrical resistivity decreases insignificantly at the same temperature. Local minimum of hardness at 200 °C coincides with increase in resistivity around 180 °C. After annealing at higher temperatures HV slowly decreases with exception of small hardening peak centered at 370 °C which occurs just before local minimum in electrical resistivity.

Electrical resistivity of as cast WEQ421 exhibits increase in the range from 160 °C to 260 °C followed by minimum at 360 °C. Resistivity increases at higher annealing temperatures and reaches maximum at 500 °C. Microhardness of as cast WEQ421 alloy slowly decreases with increasing annealing temperature in general. Small hardening peak occurs at 220 °C just before electrical resistivity plateaus at 260 °C. Slope of hardness decrease increases at high temperatures where electrical resistivity starts to rise sharply. No significant change of hardness was observed around 330 °C where resistivity strongly decreases.

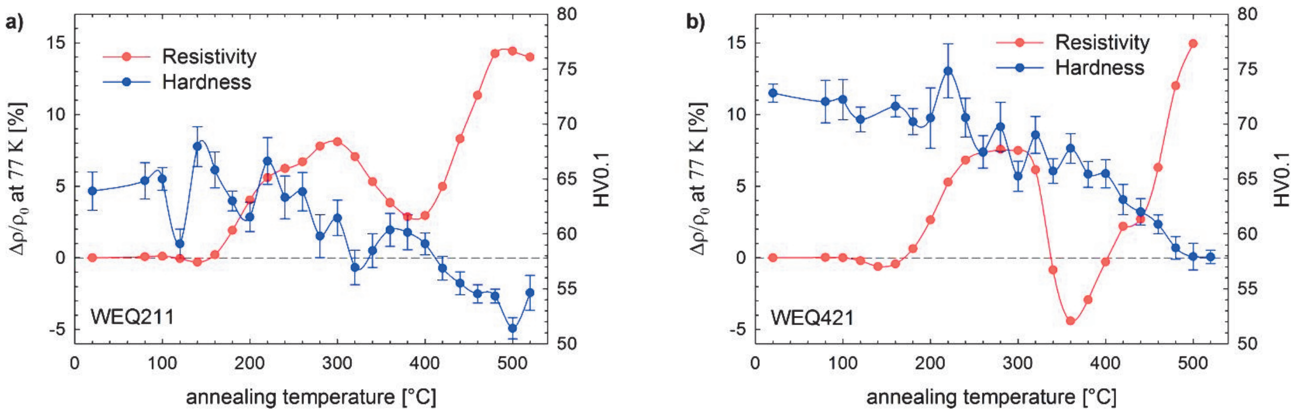

Fig. 3 Relative resistivity changes and microhardness development of as cast samples subjected to isochronal annealing: a) WEQ211, b) WEQ421

DSC measurements of as cast WEQ211 and WEQ421 samples are shown in **Fig. 4a**. DSC curve of WEQ211 alloy shows only small changes in the heat flux while DSC curve of WEQ421 alloy exhibits more pronounced changes. However, unambiguous identification of exothermic and endothermic processed based solely on DSC data is not possible for either alloy.

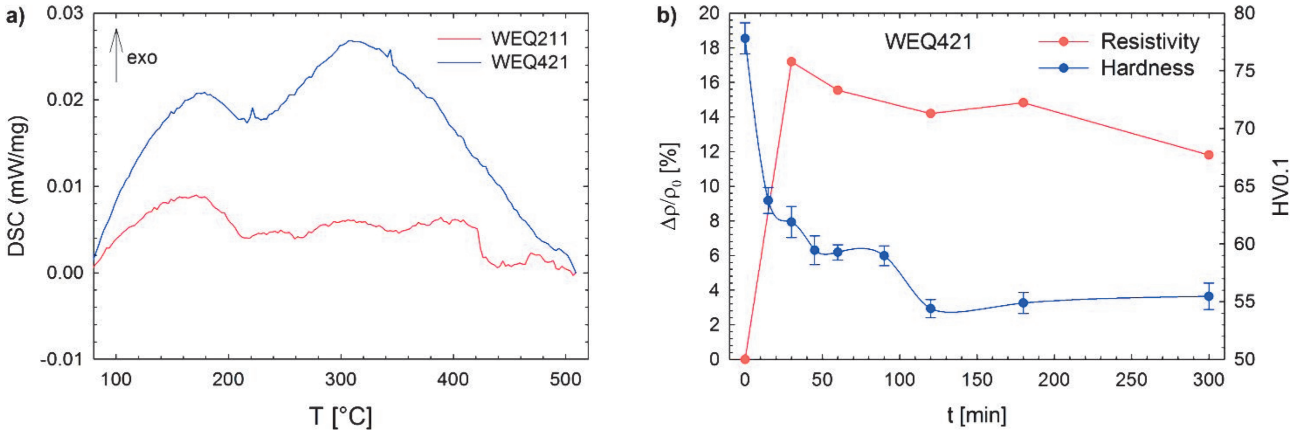

Fig. 4 a) DSC measurements of as cast alloys. Linear curve was subtracted from raw data for better visualization. b) Relative resistivity changes at 77 K and microhardness development during isothermal annealing of WEQ211 and WEQ421 alloys at 500 °C

Heat treatment of WEQ421 at 500 °C gradually dissolves almost all particles of secondary phases and concentration of solute atoms in the matrix becomes homogenous, see **Fig. 1b**. However, angular particles of Y and Nd oxides persist and there are still few remaining particles containing undissolved alloying elements. Relative resistivity and microhardness changes due to isothermal annealing at 500 °C are shown in **Fig. 4b**. Electrical resistivity sharply increases after 30 min of annealing and then slowly decreases with annealing time. Microhardness significantly decreases after 15 min of annealing and then decreases only slightly during further annealing. Therefore, annealing time of 30 min corresponding to maximum in electrical resistivity was selected for homogenization treatment. Isothermal heat treatment of WEQ211 alloy was studied in [5] and shows similar behavior as WEQ421 but the decrease in electrical resistivity with increasing annealing time is slightly lower. Annealing time of 90 min at 500 °C was found to be suitable for homogenization treatment of the WEQ211.

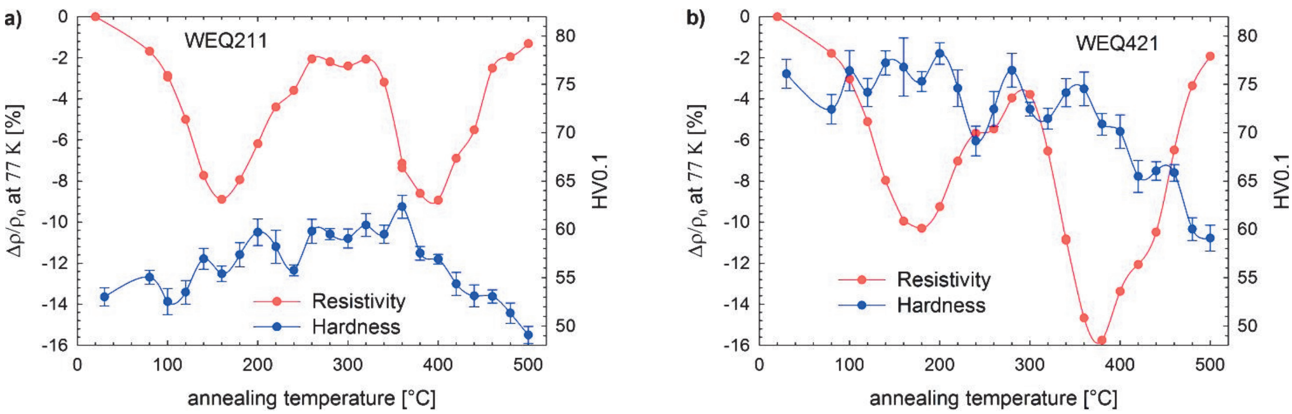

Fig. 5 Relative resistivity changes and microhardness development of homogenized samples subjected to isochronal annealing: a) WEQ211, b) WEQ421.

Homogenized samples of WEQ211 and WEQ421 alloys were also subjected to isochronal annealing. Results of microhardness and electrical resistivity measurements are shown in **Fig. 5**. Electrical resistivity of homogenized WEQ211 alloy (see **Fig. 5a**) exhibits two pronounced minima at 160 °C and 400 °C. Maximum of resistivity was reached at 500 °C but resistivity stays below its original value during whole isochronal annealing. Microhardness of homogenized WEQ211 alloy has largely increasing trend up to maximum at

360 °C which coincides with sharp decrease of resistivity around 350 °C. After annealing at higher temperatures hardness decreases and reaches minimum at 500 °C.

Electrical resistivity of homogenized WEQ421 alloy (**Fig. 5b**) shows two marked minima at 180 °C and 380 °C. Resistivity increases significantly as annealing temperature approaches 500 °C but relative resistivity changes stay below zero during whole isochronal annealing. Microhardness of homogenized WEQ421 sample is approximately constant up to annealing temperature of 200 °C despite significant decrease of resistivity. Local minimum of hardness at 240 °C is accompanied by increase of resistivity. Hardness at annealing temperatures higher than 300 °C decreases with an exception of hardening peak at 360 °C which coincides with sharp decrease of resistivity around 340 °C. Hardness decrease is significant at temperatures above 400 °C where electrical resistivity strongly grows.

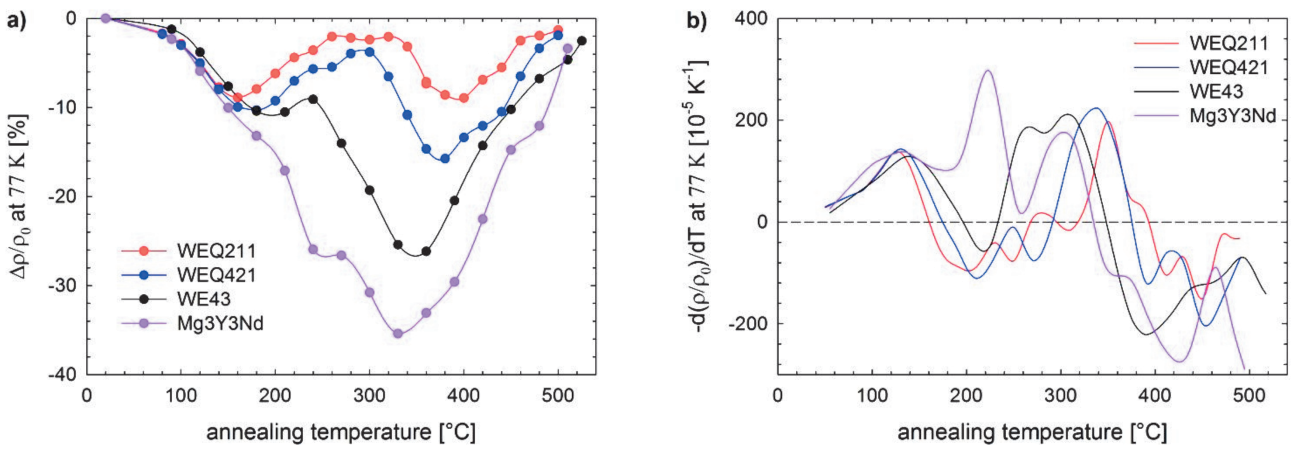

Fig. 6 Comparison of electrical resistivity measurements of WEQ211 and WEQ421 alloys with results obtained on WE43 and Mg3Y3Nd in [6]: a) relative resistivity changes, b) negative numerical derivatives of electrical resistivity

4. DISCUSSION

Results obtained on as cast and homogenized WEQ211 and WEQ421 alloys reveal complex behavior of mechanical properties. At some annealing temperatures hardness increases while electrical resistivity decreases which points to the precipitation hardening mechanism. On the other hand, at several points opposite effect was observed: hardness increases with increasing electrical resistivity which suggests solid solution hardening mechanism. Hence, both solution and precipitation hardening are competing effects and play important role in mechanical properties of studied materials. Higher concentration of solutes in WEQ421 alloy results in significantly improved hardness. The difference is especially pronounced during isochronal annealing of homogenized alloys up to 350 °C.

DSC curves were measured at higher heating rate (10 K/min) than effective heating rate of isochronal annealing (1 K/min) used for measurements of HV and electrical resistivity. Therefore, precipitation and dissolution processes should be shifted to higher temperatures in DSC data according to the Kissinger equation. Although behavior of DSC curve of as cast WEQ211 alloy shows changes at similar temperatures to changes in electrical resistivity (when the shift is taken into account) complicated nature of both curves does not permit reliable assignment of processes observed by DSC to processes measured by electrical resistivity. Minimum present on DSC curve of as cast WEQ421 alloy around 220 °C can be tentatively identified as endothermic process associated with increase of resistivity at similar temperature. However, further investigation is needed confirm this hypothesis and elucidate precipitation processes in both alloys.

Comparison of measurement of electrical resistivity on homogenized WEQ211 and WEQ421 alloys with results obtained on solution treated WE43 and Mg3Y3Nd in [6] is shown in **Fig. 6**. Negative numerical derivatives of electrical resistivity (**Fig. 6b**) can be used to depict more clearly the temperature at which resistivity changes. Evolution of electrical resistivity of homogenized WEQ211 and WEQ421 alloys up to 240 °C is similar in some features to the solution treated WE43 alloy. Plates of ordered hexagonal phase $D0_{19}$ were observed in WE43 and Mg3Y3Nd alloys annealed at 240 °C [6]. Therefore, formation of the same phase may occur in WEQ211 and WEQ421 alloys. However, one cannot exclude that solid solution decomposes according to different precipitation sequence, e.g. Mg-Ag-Nd sequence present in QE22 alloy [7]. Additionally, presence of Ag in Mg decreases stacking fault energy which enables LPSO formation in the as cast WEQ211 alloy [5]. The differences between WE43 and WEQ alloys, caused by various Y/Nd ratio and addition of Ag, become more pronounced at higher annealing temperatures. Most evident change is that the strong decrease of resistivity is shifted to higher temperature by approximately 50 °C. Investigation of microstructure of samples subjected to isochronal annealing by TEM will be necessary to identify precipitation sequence observed in studied alloys and to determine structures of the formed phases.

CONCLUSIONS

Studied WEQ211 and WEQ421 alloys offer large range of achievable hardness values which can be exploited for application specific tuning of mechanical properties. Measurements of electrical resistivity revealed that amount of alloying elements dissolved in Mg matrix can be adjusted by suitable heat treatment. This suggests that corrosion behavior can be also tailored by concentration of solutes and corresponding heat treatment.

Behavior of electrical resistivity of homogenized alloys is similar to the solution treated WE43 alloy at temperatures up to 240 °C. Therefore, $D0_{19}$ phase from Mg-Y-Nd decomposition sequence is presumably formed after annealing at 240 °C like in the solution treated WE43 alloy. However, decomposition according to different sequence (e.g. Mg-Ag-Nd) and effect of lowering stacking fault energy by Ag on phase transformations cannot be excluded. Further investigation is needed to definitively identify the precipitation sequence and structures of metastable and stable phases developed in WEQ211 and WEQ421 alloys.

ACKNOWLEDGEMENTS

The research leading to these results has received funding from the People Programme (Marie Curie Actions) of the European Union's Seventh Framework Programme FP7/2007-2013/ under REA grant agreement No. 289163.

REFERENCES

[1] WITTE, F. The history of biodegradable magnesium implants: A review. Acta Biomaterialia, 2010, Vol. 6, Issue 5, pp. 1680-1692.

[2] TIE, D., FEYERABEND, F., MÜLLER, W.D., SCHADE, R., LIEFEITH, K., KAINER K.U., WILLUMEIT, R. Antibacterial biodegradable Mg-Ag alloys. European Cells and Materials, 2013, Vol. 25, pp. 284-298.

[3] SMOLA, B., STULÍKOVÁ, I., ČERNÁ, J., ČÍŽEK, J., VLACH, M. Phase transformations in MgTbNd alloy. Physica Status Solidi (a), 2011, Vol. 208, p. 2741.

[4] POLMEAR, I.J., Light Alloys: Mettalurgy of the Light Metals. Third Edition, Butterworth-Heinemann, Oxford, UK, 1995, 204 p.

[5] LUKÁČ, F., VLČEK, M., STULÍKOVÁ, I., SMOLA, B., KUDRNOVÁ, H., VLACH, M., KEKULE, T., SZAKÁCS, G., HORT, N., KAINER, K.U. Magnesium alloy containing silver for degradable biomedical implants. In Metal 2014, submitted.

[6] VLACH, M., SMOLA, B., CÍSAŘOVÁ, H., STULÍKOVÁ, I. Precipitation Processes in Mg-Y-Nd Alloys. Defect and Diffusion Forum, 2013, Vol. 334-335, pp.155-160.

[7] KIEHN, J., SMOLA, B., VOSTRÝ, P., STULÍKOVÁ, I., KAINER, K.U. Microstructure changes in isochronally annealed alumina fibre reinforced Mg-Ag-Nd-Zr alloy. Physica Status Solidi (a), 1997, Vol. 164, pp. 709-723.